

Electron-beam-induced domain poling in LiNbO_3 for two-dimensional nonlinear frequency conversion

Yinnon Glickman, Emil Winebrand, Ady Arie,^{a)} and Gil Rosenman

Department of Physical Electronics, School of Electrical Engineering, Tel-Aviv University, Tel-Aviv, Israel 69978

(Received 16 June 2005; accepted 4 November 2005; published online 3 January 2006)

A bulk of LiNbO_3 was periodically poled in two dimensions to achieve noncollinear second-harmonic generation. The sample was fabricated using an electron-beam indirect exposure. This method used a dielectric buffer layer deposited on LiNbO_3 Z^- -polar face to trap the incident electrons. These localized electrons formed a charge droplet which generated a strong electric field and triggered the domain inversion process in the LiNbO_3 . Tailored two-dimensional domain configurations enabled quasi-phase-matched frequency doubling of a Nd:YLF laser at 15 different input angles. The measured angular dependence was in agreement with calculations based on the nonlinear reciprocal lattice vectors of the poled structure. © 2006 American Institute of Physics. [DOI: 10.1063/1.2159089]

Several techniques have been studied in recent years to obtain periodic domain inversion in ferroelectric crystals, mainly for nonlinear quasi-phase-matched frequency conversion. These techniques include for example electron-beam poling,¹ electric-field poling,² and high-voltage atomic force microscope (AFM).³ In this research, we applied a modified method of electron-beam poling.⁴ It is based on domain inversion by indirect electron-beam exposure. Electron-beam irradiation method has been used in the past for spatial modulation of nonlinear optical susceptibility coefficient $\chi^{(2)}$ but with limited success. We modified this method by coating the LiNbO_3 sample with a thin dielectric material possessing very high trap concentration that enables incident electrons localization in highly limited volume in the layer, see Fig. 1. As a result, the trapped charge was captured in the dielectric layer above the crystal and generated electric field strong enough to cause the domain inversion in the LiNbO_3 bulk. The inverted domains have a needlelike shape, with a domain diameter below $1 \mu\text{m}$ and length of up to $350 \mu\text{m}$ in the crystals' Z direction. The fabrication process is significantly shorter and straightforward than the electric-field poling process, since the mask production, photolithography, electrode deposition, and high-voltage poling steps are not needed here.

We applied the indirect electron-beam poling method for two-dimensional rectangular periodic poling of LiNbO_3 . Nonlinear frequency conversion in two-dimensionally poled structures⁵ offers several important advantages with respect to the traditional one-dimensional poling, such as much larger selection of phase matching wave vectors, possibility for simultaneous multiple-wave harmonic generation⁶ as well as realization of all-optical deflectors and splitters.⁷ The device we have fabricated was used for noncollinear second-harmonic generation of a Nd:YLF laser. By changing the entrance angle of the beam, we have observed 15 different cases of quasi-phase matching. The relations between the input and output angles enabled us to reconstruct the reciprocal lattice of the poling pattern.

The indirect electron-beam poling method was tested by poling a sample of LiNbO_3 with a rectangular lattice pattern, having periods of $14.2 \mu\text{m}$ and $13.1 \mu\text{m}$ (denoted Δx and Δy , respectively) on two perpendicular axes. The lattice motive was a circle with a diameter of $\sim 2 \mu\text{m}$. This poled lattice had dimensions of $800 \times 800 \mu\text{m}$. A $500 \mu\text{m}$ thick Z^- -cut LiNbO_3 was first coated with $2 \mu\text{m}$ dielectric layer of Shipley S-1818 photoresist using a spin coating process. The electron-beam poling was performed in a scanning electron microscope (JEOL 6400), which was adapted for electron-beam lithography machine using Raith Quantum kit. We applied acceleration voltage of 15 kV , under a charge dose of $500 \mu\text{C}/\text{cm}^2$. Using a beam current of 0.3 nA , the fabrication of single device $800 \times 800 \mu\text{m}$ lasted approximately 25 min. Figure 2(a) shows a microscope picture of the $-Z$ surface, after selective etching. Detailed study of the circular motive shows that it consists of a cluster isolated dots. Each dot motive represents an inverted domain. Its typical diameter is below 1 micron [Fig. 2(b)]. This sets the size of the smallest macrodomain that can be poled using this technique. These domains penetrate up to a thickness of ~ 350 microns into the bulk crystal. The shape of inverted domains [Fig. 2(b)] is quite different than what is observed in electric-field poling.² In electric-field poling, any inverted domain is an homogeneously polarized region. In the developed indirect electron-beam method any large inverted domain is composed from numerous nanodomain wires. Such nanodomain

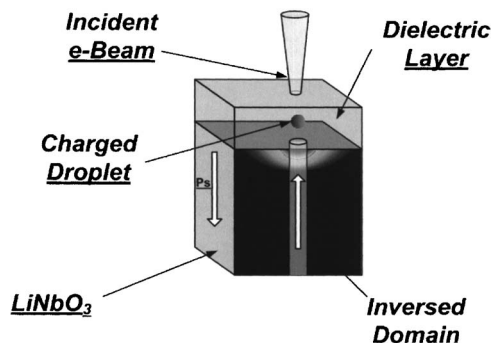


FIG. 1. Indirect electron-beam poling through a dielectric buffer layer.

^{a)}Electronic mail: ady@eng.tau.ac.il

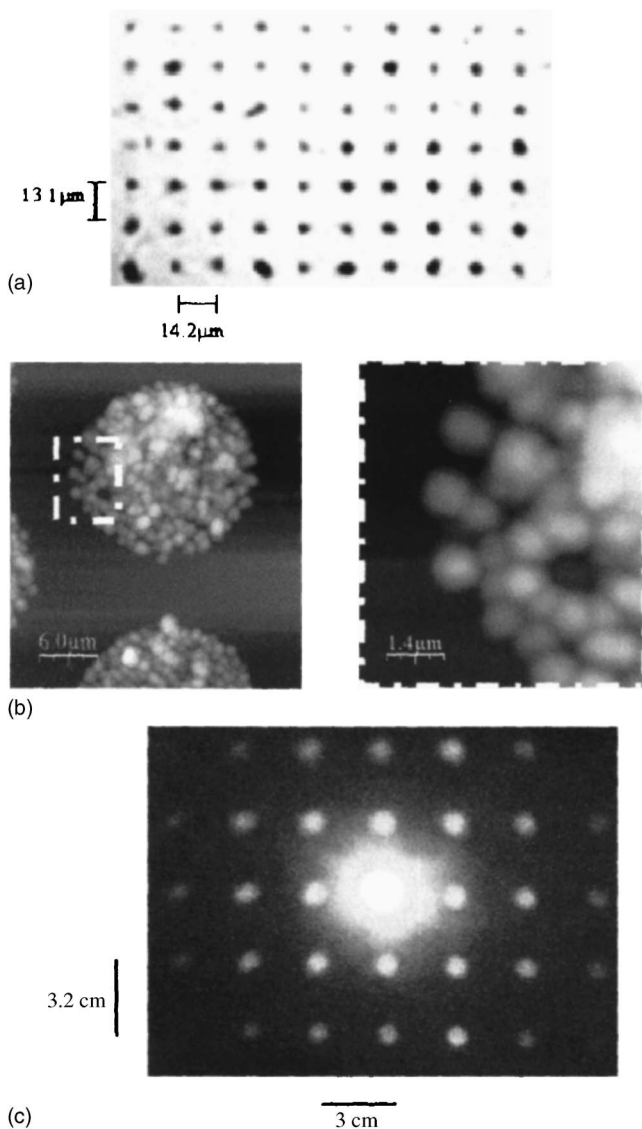


FIG. 2. (a) Microscope picture of the $-Z$ side of the etched structure, the dark dots are the inverted domains. (b) An AFM scan of a lattice node, taken from a different sample with a hexagonal poling pattern and macrodomain diameter of $\sim 18 \mu\text{m}$. The brighter shade represents deeper topography. (c) Diffraction pattern of the lattice. The bright central spot is the zeroth-order diffraction of the 532 nm beam.

wires observed in the developed indirect electron-beam poling⁴ may offer improvements in poling resolutions, although this feature of the method requires further study.

It should be noted that currently, the electron-beam poling method suffers from a charging problem of the resist layer. This Coulomb deflection of the beam leads to inaccuracies in the resulting poling pattern. Research is being carried to minimize this effect, but currently this effect limits the resolution of the patterns that can be poled in periods larger than $10 \mu\text{m}$.

The poled and etched sample was first tested by measuring the far field diffraction of a 532 nm laser beam that passed through the Z direction. The selective etching process created a small difference ($\sim 100 \text{ nm}$) between the thickness of the positive and negative domains. Hence, the phase of the optical beam was periodically modulated by the structure, and its far-field diffraction pattern became proportional to the Fourier transform of the poling pattern. Figure 2(c) shows the diffraction image on a screen placed 69 cm away from

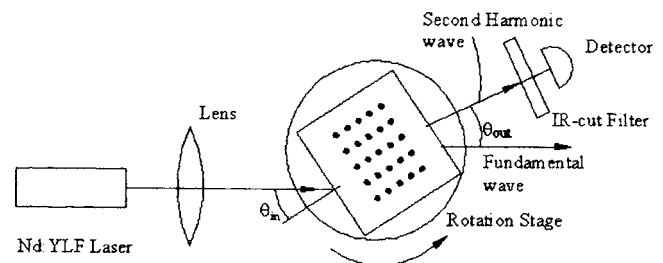


FIG. 3. Experimental setup for characterizing angle-dependent second-harmonic generation in rectangular-poled LiNbO_3 .

the sample. As expected, this image also exhibited rectangular periodicity.

The nonlinear behavior of the sample was measured⁶ using the experimental setup shown in Fig. 3. The pump source was a Lightwave Electronics 110 Nd:YLF laser ($1.047 \mu\text{m}$ wavelength) with pulse energy, repetition rate, and duration of $\sim 84 \mu\text{J}$, 1 kHz, and 6.7 ns, respectively. The Z -polarized laser light was focused to a waist radius of $30 \mu\text{m}$ in the middle of the sample. The sample itself was mounted on a rotateable stage, and was held at a temperature of 150°C , in order to avoid photorefractive damage. When the sample was rotated, fifteen angles were observed in

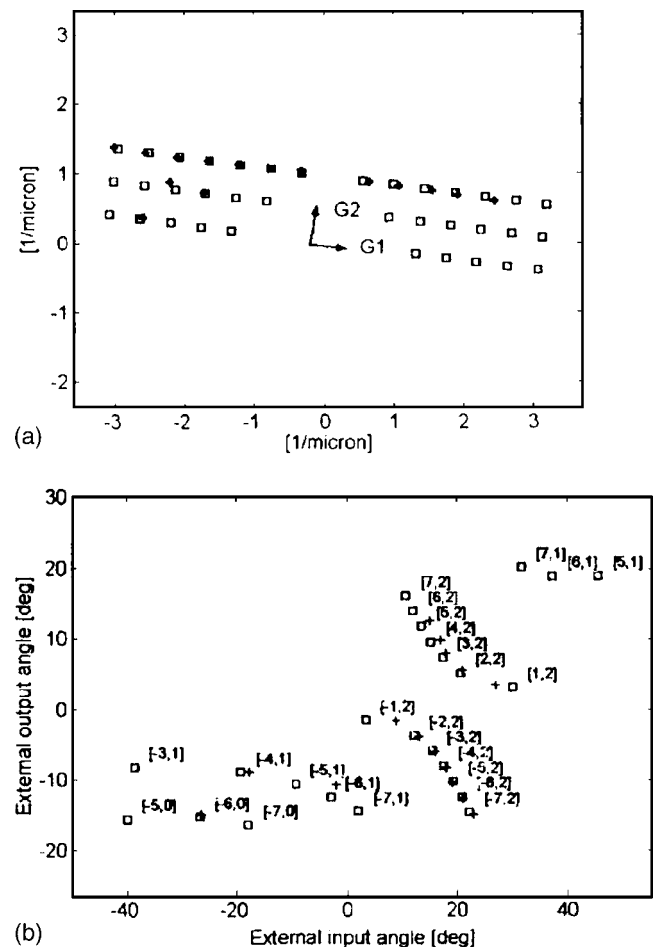


FIG. 4. (a) The reciprocal lattice for the structure. It can be noticed that both the real and the reciprocal lattices are rotated in 7.5° relative to the zero angle of the fundamental. (b) Angular relation between the fundamental input angle and the second-harmonic output angle (relative to the fundamental), both in air. In both figures, experimental values are denoted by crosses, theoretical values by squares, and the numbers in parentheses are the m and n coefficient of the corresponding RLV.

which a bright and sharp second-harmonic beam appeared on a screen in front of the sample. We have measured the input angle of the fundamental wave and the output angle of the second-harmonic wave, and using Snell law translated them to angles inside the crystal. These angles represent the directions of the fundamental and second-harmonic wave vectors. The vector quasi-phase-matching condition in this case is:

$$\mathbf{k}_{2\omega} - 2\mathbf{k}_{\omega} = m\mathbf{G}_1 + n\mathbf{G}_2, \quad (1)$$

where \mathbf{G}_1 and \mathbf{G}_2 are base vectors of the reciprocal lattice.⁵ The nodes of the reciprocal lattice are defined by the reciprocal lattice vectors (RLVs). Figure 4(a) shows the obtained vectors in the reciprocal lattice, as derived directly from the measurements of the input and output angles. As expected, these vectors exhibited rectangular periodicity, and the size of the vectors was in agreement with the measured periods in real space. Note that the lattice was rotated by 7.5° . A direct observation of the real lattice confirms this rotation with respect to the crystal input (and output) faces.

Figure 4(b) shows a comparison between the experimentally measured angles, and the calculated angles based on the relation:

$$\lambda^{2\omega} = \frac{2\pi}{|G|} \sqrt{\left(1 - \frac{n^\omega}{n^{2\omega}}\right)^2 + 4\frac{n^\omega}{n^{2\omega}} \sin^2 \theta}, \quad (2)$$

where $\lambda^{2\omega}$ is the second-harmonic wavelength inside the material, n^ω and $n^{2\omega}$ are the material index of refraction for the fundamental and the second-harmonic, respectively, and θ is one-half of the walk-off angle between the fundamental and the second harmonic. It is interesting to note that most of the measured interactions shared the same contribution of the \mathbf{G}_2 wave vector (namely, $n=2$).

We measured the second-harmonic power for several RLVs. The average power achieved by generating a second-harmonic using the $[-1, 2]$ RLV was $0.78 \mu\text{W}$. The conversion efficiency of using this RLV was 1.46×10^{-5} . In order to

estimate the theoretical expected conversion efficiency, we used a beam propagation simulation, which takes into account the Gaussian shape of the fundamental beam and the noncollinearity between the fundamental and second-harmonic beams. The calculated efficiency for the described poling pattern was 9.91×10^{-4} . We believe that the lower experimental conversion efficiency with respect to theoretical predictions was caused by irregularities of the poling pattern, the nonsmooth domain boundary shapes, and variations in the inverted domain radius.

In summary, in this letter, we demonstrated a new method for poling ferroelectric materials by indirect electron-beam irradiation. The poled structures consisted of clusters of thin stringlike inverted domains. This shape was quite different than what is observed in other poling methods, such as electric-field poling. We have shown that the method is potentially suitable for two-dimensional quasi-phase-matched second-harmonic generation, although the conversion efficiency was lower than expected owing to irregularities of the poled structure. Finally, we have shown that the reciprocal lattice vectors can be derived from the angular relations between the fundamental and harmonic waves.

This work was supported by the Israeli Ministry of Science and by the Israel Science Foundation (Grant No. 960/05).

¹M. Yamada and K. Kishima, *Electron. Lett.* **27**, 828 (1991).

²L. M. Myers, R. C. Eckardt, M. M. Fejer, and R. L. Byer, *J. Opt. Soc. Am. B* **12**, 2102 (1995).

³G. Rosenman, P. Urenski, A. Agronin, Y. Rosenwaks, and M. Molotskii, *Appl. Phys. Lett.* **82**, 103 (2003).

⁴G. Rosenman and E. Winebrand, U.S. Provisional Patent Application No. 60/634,988 (2004).

⁵V. Berger, *Phys. Rev. Lett.* **81**, 4136 (1998).

⁶N. G. R. Broderick, G. W. Ross, H. L. Offerhaus, D. J. Richardson, and D. C. Hanna, *Phys. Rev. Lett.* **84**, 4345 (2000).

⁷S. M. Saltiel and Y. S. Kivshar, *Opt. Lett.* **27**, 921 (2002).